Effect of Cross-Link Density on Interphase Creation in Polymer Nanocomposites

Karl W. Putz,[†] Marc J. Palmeri,[‡] Rachel B. Cohn,[§,⊥] Rodney Andrews,[||] and L. Catherine Brinson*[,†,‡]

Department of Mechanical Engineering, Department of Materials Science and Engineering, and MRSEC−REU Program, Northwestern University, Evanston, Illinois 60208, and Center for Applied Energy Research, University of Kentucky, Lexington, Kentucky 40506

Received April 14, 2008; Revised Manuscript Received July 14, 2008

ABSTRACT: The thermal and dynamic behavior of epoxy nanocomposites with varying cross-link density was tested via dynamic scanning calorimetry (DSC) in order to determine the influence of cross-link density on the creation of "interphase", zones of altered polymer properties near polymer−particle interfaces. The results show that the inclusion of nanoparticles creates an increase in the glass transition temperature (T_g) at low cross-link density and a decrease in T_g at higher cross-link densities. This phenomenon suggests that two mechanisms work in tandem to alter the T_g of epoxy systems, with relative magnitudes determined by cross-link density: (1) network disruption at the nanotube−polymer interfaces leading to lower T_g and (2) interphase creation leading to retarded dynamics, resulting in higher T_g. Results show that as cross-link density increases, the length scale of cooperatively rearranging regions (CRRs) decreases. This decrease hinders communication of the dynamics between adjacent CRRs, thereby reducing interphase penetration into the bulk matrix. Moreover, increasing cross-link density leads to increased network disruption due to the presence of nanoparticle obstacles in an otherwise densely connected network.

Introduction

Recent work in polymer nanocomposites has demonstrated that incorporation of very small weight fractions of nanoparticles has the ability to significantly alter bulk polymer properties.[1−4] While some of the changes are due to the inherent properties of the nanoparticles themselves, alterations in the glass transition temperature indicate fundamental changes in polymer mobility due to the interaction of polymer chains with the nanoparticle surfaces. This region of the polymer matrix, in which interactions with the nanoparticle surfaces substantially modify the chain dynamics and properties, is typically termed the interphase. Sheathing of polymers around nanotubes on fracture surfaces provides strong visual evidence of this phenomenon.[5] While small interphase regions exist in traditional composites with micron-scale filler dimensions, the interphase is of critical importance for nanocomposites due to the extraordinarily high surface area to volume ratio of nanoparticles. In well-dispersed systems, it is possible for the interphase zones to percolate through the entire nanocomposite, thus dominating bulk properties.[1−4] Such a percolated interphase network manifests itself through changes in bulk properties such as the glass transition temperature (T_g), aging response, and modulus.[3,4,6,7]

The small interparticle distances in nanocomposites and associated T_g changes relative to the neat matrix (no nanoparticles) have been quantitatively linked to confinement effects on T_g in thin polymer films.[1,8] In thin films, the length scale of the confinement effect (50−500 nm) is larger than and independent of the radius of gyration (R_g) of most polymer chains.[8,9] One theory that may explain the mismatched length scales involves the concept of cooperatively rearranging regions (CRRs) from the Adam−Gibbs model of the glass transition. Since the polymer chain system is densely packed, center-of-mass motions (glass transition) of one chain segment necessarily involve coordinated motions of other segments. The length scale of these coordinated motions can be measured by various means[10−13] and is typically in the range of 2−4 nm for polymeric systems. While these domains are usually smaller in length scale compared with R_g, the CRRs are not discrete; thus, the dynamics of one CRR affect neighboring regions. In this way, a strong polymer−substrate interaction will affect the dynamics of the nearest layer of polymer segments, and the change in dynamics can be propagated up to several hundred nanometers into a film.

Quantitative studies on confinement in thin polymer films have been performed only on thermoplastic systems. However, nanocomposites with thermoset matrices have also been explored, particularly cross-linked epoxy matrices for usage in many structural applications. While no specific assessment of confinement or interphase effects have been discussed for these nanocomposites, several examples of increased T_g in epoxies through the incorporation of nanoparticles can be found in the literature.[14−19] In many cases,[15,17,19] functionalization of the nanotubes has resulted in strong (covalent) interactions and thus retarded surface dynamics, resulting in a substantial interphase regime as described above. However, many examples of depressed T_g in epoxies due to nanotube inclusion may also be found.[14,16−18,20] Little discussion is offered regarding the mechanism behind these T_g decreases or the apparent discrepancies between results on the same nominal system of an epoxy matrix with carbon nanotube filler. Additionally, there are no data in the literature showing improved T_g with nanotubes for high-performance epoxies. Thus, interphase-like behavior with associated T_g increases in nanoparticle-filled epoxy systems has only been found in particular cases of epoxies with relatively low glass transition temperatures (<150 °C).

A fundamental difference between low- and high-performance epoxies is the density of covalent cross-links within the network. General agreement attributes increases in glass transition temperature with cross-link density to the limitations in chain

* To whom correspondence should be addressed.
[†] Department of Mechanical Engineering, Northwestern University.
[‡] Department of Materials Science and Engineering, Northwestern University.
[§] MRSEC−REU Program, Northwestern University.
[||] University of Kentucky.
[⊥] Currently at Brown University.

10.1021/ma800830p CCC: $40.75
Published on Web 08/26/2008

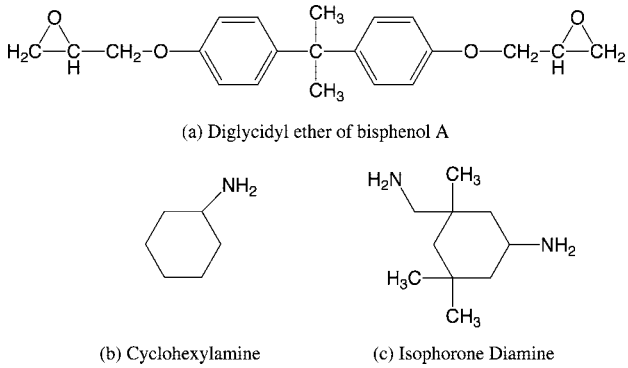

Figure 1. Chemical structures of (a) diglycidyl ether of bisphenol A (DGEBA) resin, (b) cyclohexylamine (CHA) chain extender, and (c) isophorone diamine (IPD) cross-linker.

mobility due to the presence of the cross-links. In neat epoxy resin systems, several approaches have been used to study the influence of cross-linking on molecular scale dynamics using systems based on an epoxide resin cured with a hardener containing amine functional groups. These methods include varying the curing time or temperature in order to produce systems with different degrees of cross-linking,[21] altering the molecular weight between cross-links by changing the molecular weights of the epoxide or amine chains,[22,23] or by altering the reactive group functionality of the curing agent. A model system for this last method includes diglycidyl ether of bisphenol A (DGEBA) resin cured with various combinations of monoamine "chain extender" and diamine "cross-linker" chains while keeping the epoxide/amine stoichiometry constant.[24−26] This method is particularly attractive for investigating the cross-link density without added compositional variation.[27]

In this work, we apply this method to polymer nanocomposites and systematically study the difference between interphase formation near nanoparticles in a linear polymer resin and in progressively cross-linked polymer networks. To achieve this end, we disperse unfunctionalized multiwalled carbon nanotubes (MWNTs) in varied blends of a difunctional epoxide resin with mono- and difunctional amines. This method was selected to vary cross-link density without changing the ratio of functional groups, thus minimizing changes in the interaction strength between the matrix and the MWNTs. T_g was measured using dynamic scanning calorimetry (DSC) to detect the signature of interphase formation. Interphase behavior (and increasing T_g) is demonstrated for linear chains and sparsely cross-linked systems but vanishes as cross-link density increases. Further DSC studies were performed to understand the underlying trends.

Methods

Diglycidyl ether of bisphenol A (DGEBA, Sigma-Aldrich), cyclohexylamine (CHA, Sigma-Aldrich), and isophorone diamine (IPD, Sigma-Aldrich) were used to make nanocomposite samples (Figure 1). The epoxide to amine stoichiometry was kept constant at 2:1. MWNTs produced by CVD with a diameter of ∼25 nm were used as the nanofiller material. Surface analysis by XPS found carbon with small amounts of oxygen (<2 mol %), thus confirming the unfunctionalized aromatic surface.

The cross-link density is defined by the diamine fraction, Ξ, which represents the fraction of amine functional groups that are present in diamine molecules:

$$\Xi = \frac{2[\mathrm{IPD}]}{2[\mathrm{IPD}] + [\mathrm{CHA}]} \quad (1)$$

Ξ was varied from linear chains cured with CHA (diamine Ξ = 0) to a fully cross-linked network cured with IPD (Ξ = 1), with intermediate steps of 0.25, 0.50, and 0.75 diamine fraction. Three samples were made at each cross-link density: neat (0 wt %), 0.25 wt %, and 0.5 wt % MWNT.

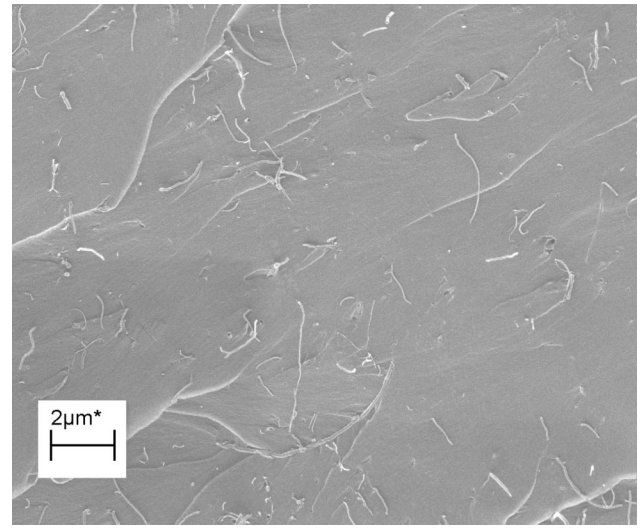

Figure 2. SEM micrograph of a sample containing 0.5 wt % MWNT and Ξ = 0.75. The sample was coated with 5 nm film of gold−palladium, and the image was captured using a magnification of 10 000× and beam energy of 1.00 kV.

Each nanocomposite sample was mixed by combining an appropriate amount of the neat masterbatch (epoxide resin + amine mixture) with nanotubes, so that all samples of a given cross-link density retained the same matrix phase composition. Blending of the nanoparticles was performed by two 2 min shear−mixing cycles at 10 000 rpm. All three samples of a given cross-link density were cured simultaneously in the same oven with the following curing cycle: 1 h at 140 °C, 6 h at 190 °C, 5 h postcure at 190 °C. The last step of postcuring was performed to ensure completion of curing.

Curing was subsequently confirmed by a 10 °C/min temperature ramp in the DSC to 320 °C where exothermal signatures indicative of incomplete curing would be observed. Dispersion of the nanotubes was checked via SEM analysis of a fracture sample. Individual tubes were observed, and large aggregates were not found, as demonstrated in Figure 2.

Samples were not well suited for mechanical testing due to porosity induced by the release of gas during the curing process. This porosity was trapped in the nanocomposite samples due to the formation of a load-bearing network from good nanotube dispersion.[28] This elastic network resulted in an increased viscosity that prevented the escape of air bubbles within the time scale of the curing reaction. Despite this macroscale porosity, high repeatability in T_g data for multiple experiments on specimens from various locations within a given sample demonstrates negligible global heterogeneity.

DSC work was performed on a Mettler Toledo DSC 822 with sample sizes between 4 and 7 mg. The glass transition temperatures reported are the midpoint T_g measured on the second cycle upon cooling at 10 °C/min after annealing at least 30 °C above T_g for 4 min. The change in the heat capacity at T_g, ΔC_p, is reported from the same experiment for each neat epoxy sample, and the length scale of the glass transition (ξ_{CRR}) was measured on the DSC by the method derived by Donth.[13,29] In practice, this involved cooling from an annealed state at 5 °C/min through the glass transition, then heating the sample at 5 °C/min through T_g, and measuring the width of the transition (in temperature) and $\Delta(1/C_p)$ as explained in the text. Sample densities were measured by helium pycnometry.

Results and Discussion

The properties of the neat samples are presented first to demonstrate the success of the method used to change cross-link density. The T_g and ΔC_p of neat samples are shown in

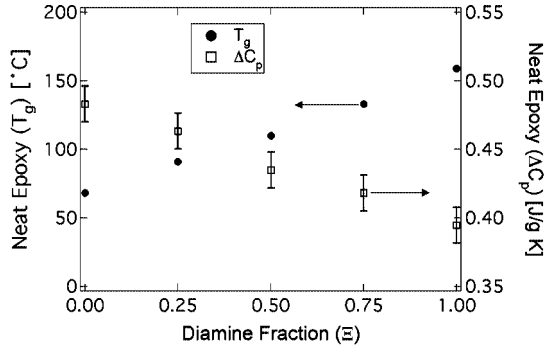

Figure 3. Glass transition temperature (T_g) and change in heat capacity (ΔC_p) of the neat epoxy samples as a function of the diamine fraction (Ξ). Error bars represent a composite standard deviation of the samples and are too small for observation for the T_g data.

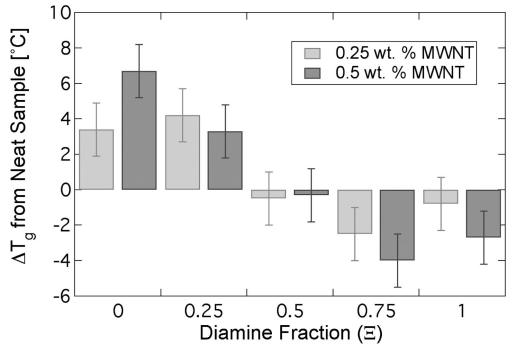

Figure 4. Difference between T_g of the nanocomposites and neat epoxy as a function of diamine fraction (Ξ). Error bars represent the combined measurement error of both neat and nanocomposite samples.

Figure 3. The T_g of the neat samples increases monotonically with diamine fraction. The relationship is in accordance with previous studies[24,25] and corroborates the intuitive reasoning that covalent cross-links restrict the mobility of polymer segments. Moreover, ΔC_p of the neat samples decreases as the fraction of diamine is increased, which agrees with previous studies.[24] ΔC_p is a byproduct of the increase in entropy gained by the system as the chains move more freely, and our results show ΔC_p decreases as cross-links increasingly restrict the conformations available to the rubbery material above T_g. Both curves are linear with $R^2 > 0.99$, which shows a surprisingly simple relationship despite the complex nature of the glass transition. Other studies of cross-link density effects in polymeric systems result in linear relationships as well,[30,31] which is amenable to current theoretical modeling.[32]

Figure 4 presents the difference in T_g between the nanocomposites and neat samples at a given diamine fraction. Nanocomposites based on purely linear polymer (Ξ = 0) show an increased T_g. The increase is approximately the same for a loosely cross-linked network (Ξ = 0.25) and then disappears completely at the midpoint (Ξ = 0.5). Highly cross-linked samples have a slightly negative ΔT_g.

We propose three possible mechanisms for alteration of T_g of the epoxy matrix by nanoparticle inclusion in Figure 5. First, altered thermal conductivity of the sample due to the nanoparticles may change the curing kinetics for a given system and thus impede attainment of a consistent cross-link density for the standard curing cycle (Figure 5b). In this work, we followed the recommended curing cycle[25] and postcured for an additional 5 h at 190 °C. All three samples at a given diamine fraction were cured simultaneously in the same oven. Additionally, the nanocomposites were created from the same masterbatch of epoxy/amine mixture as the neat samples for a given cross-link

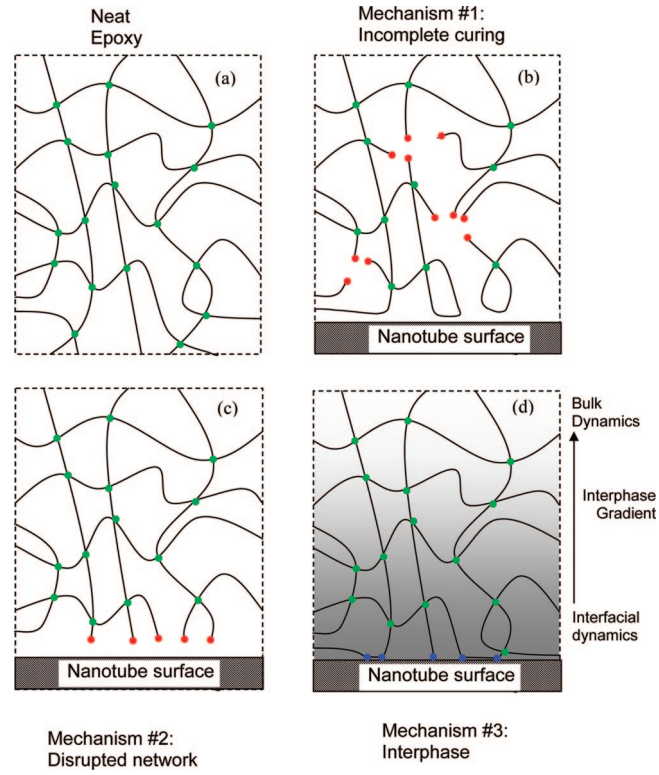

Figure 5. Schematic diagrams of the three proposed mechanisms of T_g changes in epoxy nanocomposites: (a) fully cured neat epoxy (with green dots representing covalent cross-links), (b) mechanism 1 showing dangling unreacted end groups of epoxide chains (red dots) due to incomplete curing, (c) mechanism 2 showing unreacted end groups at the nanotube surface due to nanotube-induced network disruption, and (d) mechanism 3 of interphase creation showing secondary bonding (blue dots) with the CNT surface that modifies network dynamics.

density. All samples were also checked for completion of curing by DSC, and no exothermic peaks indicative of incomplete curing were found. These precautions provide strong evidence for equal extent of curing in the samples and thus eliminate incomplete cross-linking as a plausible mechanism for a change in T_g for this particular study.

The second mechanism to explain altered T_g's in a thermoset-based nanocomposite is network disruption (Figure 5c). The epoxy network near nanoparticle interfaces may be disrupted compared to the bulk matrix, leading to an effective decrease in cross-link density and diminished T_g. We posit two possible reasons for network disruption: (1) steric limitations near interfaces and (2) phase segregation. In this work, the nanotubes are unreactive surfaces, and thus functional groups near the surface may not be able to react because the presence of the nanotube limits the number of functional groups in the local vicinity (steric limitations). Alternatively, either the amine or the epoxy may phase segregate to the nanotube interface, resulting in local functional group ratios that are not consistent with their bulk values (2:1 amine to epoxide), which would likely result in altered cross-link densities. Whether by means of steric limitations or phase segregation, this mechanism would likely lead to a decrease in T_g in the bulk matrix of the sample. Considering the results in Figure 3, network disruption is the likely cause of the statistically significant decreases in T_g observed in the highly cross-linked nanocomposites. This mechanism of network disruption may also be present at lower diamine fractions but would be smaller in magnitude and may be offset by a different mechanism that increases T_g as discussed below.

The final mechanism for T_g changes observed in epoxy nanocomposites corresponds to interphase creation, analogous

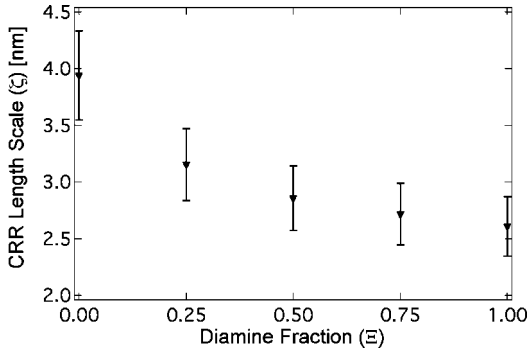

Figure 6. Cooperatively rearranging region (CRR) length scale (ζ) as a function of diamine fraction (Ξ) with composite standard deviation bars.

to the altered mobility arguments made for thin films or nanocomposites based on thermoplastic polymers. The interphase can either increase T_g by retarding the dynamics in systems via strong attractive interactions or decrease T_g through repulsive interfacial interactions. In this study, linear chains and lightly cross-linked networks have an increased T_g, an indication of an interphase characterized by positive attractions. The specific attraction in this system, composed of DGEBA epoxy and MWNTs, may be π stacking[33] between the aromatic groups in DGEBA and the surface of the MWNTs. The interphase effect is not strong in this system, producing a maximum change of only 7 °C. However, the interaction that leads to the interphase should be constant across the cross-link density series since the functional group composition is constant between linear chains and a fully formed network.

Since the underlying interaction that causes the interphase does not change with cross-link density, further investigations were undertaken to understand how cross-link density affects interphase creation by probing the inherent length scale of the glass transition (ζ). Donth et al. proposed a method using DSC to measure the CRR volume (ξ^3)

$$\xi^3 = \frac{\Delta(1/C_v)}{\rho(\delta T)^2} k_B T^2 \tag{2}$$

where ρ is the density (1.145 ± 0.01 g/cm^3 for all samples), k_B is the Boltzmann constant, T is the temperature, C_v is the heat capacity at constant volume, and $(\delta T)^2$ is the temperature fluctuation of one CRR. Details on the method can be found in papers by Donth et al.,[13,29] with an additional simplified explanation and accompanying diagram provided by Saiter et al.[34]

Figure 6 shows the characteristic length scale of the glass transition—the length of a CRR (ζ)—as a function of diamine fraction, Ξ, for the neat samples in this study. The CRR length scale for a nanocomposite of a given cross-link density was indistinguishable from (i.e., within error of) a corresponding neat sample with the same cross-link density. The CRR length was found to decrease monotonically with increasing cross-link density from 3.9 nm for linear chains to 2.6 nm for the fully cross-linked network. The volume of the cooperative motion raises these values to the third power, resulting in a CRR volume for a fully cross-linked network that is only about one-third that of a system of linear chains. This corresponds to an astonishing loss of cooperativity in the system, even though intuition may lead one to believe that covalent cross-links would increase the distances over which motions are linked.

In order to understand why the size of the CRRs shrink as the system becomes more cross-linked, consider two arguments about the relationship between connectivity and rearrangement sizes in an abstract system. In the first argument, cross-links promote relaxations over larger length scales under the straightforward assumption that two chain units linked by covalent bonds lead to motions more strongly coupled than if they are not part of the same molecule. Thus, this first argument leads to the idea that rearrangement (CRR) size should grow as network connectivity (cross-link density) increases.

The second argument, in contrast, explains that relaxation occurs over smaller length scales as cross-link density increases. In this second argument, consider that no connectivity in the system (linear chains) leads to relatively free-moving individual chain units. Large-scale motion is possible because of the lack of topological constraints. As network connectivity is increased, covalent bonds restrict the spatial rearrangements of individual chain units. Constraints imposed on the system by the cross-links increase the activation energy of large-scale chain motions and hence impede them in favor of more localized motions, thereby decreasing the CRR size with cross-link density.

The results on our system indicate that the latter argument is operative, despite the fact that it may seem less intuitive. Cross-links inhibit large-scale motions in cross-linked polymers, leading to smaller CRRs. This relationship has not been well established in polymer systems but is documented in aggregate studies of a wide range of glass-forming materials (small organic molecules to network inorganic glasses).[35−37]

Critically, there exists a natural link between cooperativity and interphase-induced T_g changes. As stated in the Introduction, one theory of interphase formation relies on communication between the relaxing cooperative regions in order to percolate interface effects deeper into the polymer matrix. Naturally, changes in the cooperative length scale will affect the distance from the interface that the effects of an interaction will be observed. As the cooperatively rearranging regions become smaller, the length scale over which the change in dynamics is propagated from an interface also decreases. This results in a loss in the interphase behavior in polymer nanocomposites with increasing cross-link density.

In our system, we propose that the interphase mechanism and the network disruption mechanism work together in the nanocomposites to affect the T_g of the material system and that the degree of influence of each mechanism varies with cross-link density. The network disruption mechanism, resulting in decreased effective cross-link density and decreased T_g, increases in magnitude with increasing cross-link density of the matrix. In contrast, the restricted mobility interphase decreases in importance with increasing cross-link density due to the reduction in the CRR size with increasing cross-link density. Overall, the interphase effect can either mask the (small) network disruption effect in lightly cross-linked systems or is itself diminished and also counteracted by network disruption in highly cross-linked systems.

Conclusion

In this paper, we systematically varied cross-link density in order to understand its effect on the formation of an interphase in cross-linked nanocomposite systems. Three mechanisms of T_g variation were proposed in order to explain the interactions of cross-linked polymer networks with nanofillers. For the system examined here, two of these mechanisms were proposed to be active. At low cross-link density, a T_g increase was measured, indicating a restricted mobility interphase formed by attractive interactions between the polymer and the nanoparticles. As the cross-link density was increased, T_g of the nanocomposites was observed to remain constant or decrease. This T_g decrease was related to two mechanisms working in tandem: First, a reduction in the cooperativity of the system with increased cross-link density was shown which translates into less communication of interfacial dynamics through the bulk

of the polymer matrix. The reduction of the extent of interphase from the nanoparticle interfaces leads to smaller or negligible impact of the interphase on glass transition. Second, the nanotubes may disrupt the cross-linking network of the system, reducing the effective cross-link density and leading to degradation in T_g. These results have important implications both for interpreting existing data in the literature of various epoxy nanocomposite systems and for design of nanocomposites in thermosetting resins. In highly cross-linked thermosets, the ability of nanoparticles to significantly alter the physical and thermal properties of the polymer through creation of a percolated interphase of altered polymer matrix properties will be significantly decreased.

Acknowledgment. The authors gratefully acknowledge support from The Ford-Boeing-Northwestern Alliance, the NSF NIRT program under Award CMS-0404291, and the NSF-MRSEC Program at Northwestern University under Grant DMR 0520513.

References and Notes

(1) Bansal, A.; Yang, H.; Li, C.; Cho, K.; Benicewicz, B. C.; Kumar, S. K.; Schadler, L. S. *Nat. Mater.* **2005**, *4*, 693–698.
(2) Putz, K.; Krishnamoorti, R.; Green, P. F. *Polymer* **2007**, *48*, 3540–3545.
(3) Putz, K.; Mitchell, C. A.; Krishnamoorti, R.; Green, P. F. *J. Polym. Sci., Part B: Polym. Phys.* **2004**, *42*, 2286–2293.
(4) Ramanathan, T.; Liu, H.; Brinson, L. C. *J. Polym. Sci., Part B: Polym. Phys.* **2005**, *43*, 2269–2279.
(5) Ding, W.; Eitan, A.; Fisher, F. T.; Chen, X.; Dikin, D. A.; Andrews, R.; Brinson, L. C.; Schadler, L. S.; Ruoff, R. S. *Nano Lett.* **2003**, *3*, 1593–1597.
(6) Flory, A.; Shull, K.; Brinson, L. C. Manuscript in preparation.
(7) Lu, H. B.; Nutt, S. *Macromolecules* **2003**, *36*, 4010–4016.
(8) Rittigstein, P.; Priestley, R. D.; Broadbelt, L. J.; Torkelson, J. M. *Nat. Mater.* **2007**, *6*, 278–282.
(9) Ellison, C. J.; Mundra, M. K.; Torkelson, J. M. *Macromolecules* **2005**, *38*, 1767–1778.
(10) Erwin, B. M.; Colby, R. H. *J. Non-Cryst. Solids* **2002**, *307*, 225–231.
(11) Hong, P. D.; Chuang, W. T.; Yeh, W. J.; Lin, T. L. *Polymer* **2002**, *43*, 6879–6886.
(12) Tracht, U.; Wilhelm, M.; Heuer, A.; Feng, H.; Schmidt-Rohr, K.; Spiess, H. W. *Phys. Rev. Lett.* **1998**, *81*, 2727–2730.
(13) Donth, E. *J. Polym. Sci., Part B: Polym. Phys.* **1996**, *34*, 2881–2892.
(14) Fidelus, J. D.; Wiesel, E.; Gojny, F. H.; Schulte, K.; Wagner, H. D. *Composites, Part A* **2005**, *36*, 1555–1561.
(15) Gojny, F. H.; Schulte, K. *Compos. Sci. Technol.* **2004**, *64*, 2303–2308.
(16) Gong, X. Y.; Liu, J.; Baskaran, S.; Voise, R. D.; Young, J. S. *Chem. Mater.* **2000**, *12*, 1049–1052.
(17) Zhamu, A.; Hou, Y. P.; Zhong, W. H.; Stone, J. J.; Li, J.; Lukehart, C. M. *Polym. Compos.* **2007**, *28*, 605–611.
(18) Liao, Y. H.; Marietta-Tondin, O.; Liang, Z. Y.; Zhang, C.; Wang, B. *Mater. Sci. Eng., A* **2004**, *385*, 175–181.
(19) Wang, J. G.; Fang, Z. P.; Gu, A. J.; Xu, L. H.; Liu, F. *J. Appl. Polym. Sci.* **2006**, *100*, 97–104.
(20) Miyagawa, H.; Drzal, L. T. *Polymer* **2004**, *45*, 5163–5170.
(21) Varley, R. J.; Hodgkin, J. H.; Simon, G. P. *J. Appl. Polym. Sci.* **2000**, *77*, 237–248.
(22) Plazek, D. J.; Choy, I. C. *J. Polym. Sci., Part B: Polym. Phys.* **1989**, *27*, 307–324.
(23) Lee, A.; McKenna, G. B. *Polymer* **1988**, *29*, 1812–1817.
(24) Sindt, O.; Perez, J.; Gerard, J. F. *Polymer* **1996**, *37*, 2989–2997.
(25) Won, Y. G.; Galy, J.; Gerard, J. F.; Pascault, J. P.; Bellenger, V.; Verdu, J. *Polymer* **1990**, *31*, 1787–1792.
(26) Charlesworth, J. M. *Polym. Eng. Sci.* **1988**, *28*, 221–229.
(27) Cook, W. D.; Mehrabi, M.; Edward, G. H. *Polymer* **1999**, *40*, 1209–1218.
(28) Mitchell, C. A.; Bahr, J. L.; Arepalli, S.; Tour, J. M.; Krishnamoorti, R. *Macromolecules* **2002**, *35*, 8825–8830.
(29) Donth, E.; Korus, J.; Hempel, E.; Beiner, M. *Thermochim. Acta* **1997**, *305*, 239–249.
(30) Droger, N.; Primel, O.; Halary, J. L. *J. Appl. Polym. Sci.* **2008**, *107*, 455–462.
(31) Robertson, C. G.; Wang, X. R. *Macromolecules* **2004**, *37*, 4266–4270.
(32) Venditti, R. A.; Gillham, J. K. *J. Appl. Polym. Sci.* **1997**, *64*, 3–14.
(33) Tournus, F.; Latil, S.; Heggie, M. I.; Charlier, J. C. *Phys. Rev. B* **2005**, *72*, 07431-1–07431-5.
(34) Saiter, A.; Couderc, H.; Grenet, J. *J. Therm. Anal. Calorim.* **2007**, *88*, 483–488.
(35) Angell, C. A. *J. Non-Cryst. Solids* **1991**, *131−133*, 13–31.
(36) Boehmer, R.; Angell, C. A. *Phys. Rev. B: Condens. Matter Mater. Phys.* **1992**, *45*, 10091–4.
(37) Boehmer, R.; Ngai, K. L.; Angell, C. A.; Plazek, D. J. *J. Chem. Phys.* **1993**, *99*, 4201–9.

MA800830P